Echinocystic acid induces the apoptosis, and inhibits the migration and invasion of non-small cell lung cancer cells

duojie zhu (zhudj20@lzu.edu.cn)
Lanzhou University Second Hospital https://orcid.org/0000-0002-0183-8257
Cheng Wang
Lanzhou University Second Hospital
Peng Jiang
Lanzhou University Second Hospital
Futian Tang
Lanzhou University Second Hospital
Yumin Li
Lanzhou University Second Hospital
bin li
Lanzhou University Second Hospital

Research Article

Keywords: echinocystic acid, NSCLC, A549, Par3, apoptosis

Posted Date: February 28th, 2022

DOI: https://doi.org/10.21203/rs.3.rs-1338328/v1

Abstract

An increasing amount of evidence has demonstrated the anticancer activity of triterpenes extracted from traditional medicines. Echinocystic acid (EA), a natural triterpene isolated from *Eclipta prostrata* (L.) L., has previously been shown to exhibit anticancer activity in HepG2 and HL-60 cells. The aim of the present study was to investigate the anticancer activity of EA in non-small cell lung cancer (NSCLC) cells. For this purpose, the viability and proliferation of A549 cells were determined using a Cell Counting Kit-8 and 5-ethynyl-2′-deoxyuridine staining. The migratory and invasive ability of the A549 cells were measured using wound healing and Transwell assays. Hoechst staining was also performed to detect the apoptosis of A549 cells. The proliferation of A549 cells and the distributions of different growth phases were determined using a flow cytometer. Western blot analysis was used to detect the expression levels of cyclin D, partitioning defective 3 homolog (Par3), PI3K, Akt, mTOR, Bax, Bcl-2 and caspase-3. EA inhibited the proliferation, and the migratory and invasive abilities of cultured lung carcinoma cells (A549 cells), and induced cell cycle arrest in the G_1 phase of the cell cycle. Treatment with EA upregulated Par3 expression and inhibited the PI3K/Akt/mTOR pathway *in vitro*. In addition, EA treatment inhibited tumor growth, suppressed proliferation and induced the apoptosis of tumor cells in NSCLC tumor xenografts in mice. On the whole, these results suggest that EA may represent a potential therapeutic agent for NSCLC.

Introduction

Lung cancer is the second most frequently occurring type of cancer, with >1.6 million cases diagnosed each year. It is also associated with high morbidity and mortality rates. Tobacco consumption and exposure to environmental carcinogens are major risk factors for the development of lung cancer (1). The majority of patients present with advanced disease at the time of diagnosis, with an estimated 5-year relative survival rate of 17% (2). Lung cancer is classically subdivided into small cell lung cancer (SCLC) and three types of non-small cell lung cancer (NSCLC); NSCLC accounts for ~80% of primary lung cancers (3). Despite breakthroughs in surgical techniques and other therapies, treatment options for NSCLC remain limited. The majority of patients with NSCLC have a poor response to standard chemotherapy regimens, at least in part due to the high prevalence of multiple drug resistance (4). Therefore, affected patients urgently require the development of novel chemotherapy drugs and the establishment of novel strategies against the tumorigenesis and progression of NSCLC.

Traditional herbal medicines provide pharmacotherapy for millions of individuals worldwide, and they continue to be valuable sources for drug discovery (5). It has been reported that several classes of triterpenes extracted from traditional medicines possess anticancer and chemopreventive properties, which may be associated with their anti-inflammatory and antioxidant effects (6). Echinocystic acid (EA) (chemical structure illustrated in Fig. 1), a natural triterpene isolated from *Eclipta prostrata* (L.) L. (*E. prostrata*), has been shown to exhibit anticancer activity in human hepatoblastoma (HepG2) and human leukemia (HL-60) cells (7,8). Previous studies have demonstrated that EA constitutes the aerial parts of *E. prostrata*, and can induce the apoptosis and cytotoxicity of human endometrial cancer cells and human ovarian cancer cells (9,10). Furthermore, certain specific compounds or extracts from

E. prostrata have been shown to exert antitumor activity in Hep-G2, PC12, A549 cells (11). To the best of our knowledge, the inhibitory effects of EA on NSCLC have not yet been reported to date. However, there have been some reports on the effects of EA on respiratory disorders. Recent findings have demonstrated that EA can protect human bronchial epithelial cells against cigarette smoke extract-induced injury by modulating the nuclear factor erythroid 2–related factor 2 (Nrf2) pathway (12). EA has also been shown to inhibit lipopolysaccharide (LPS)-induced acute lung inflammation in mice, and decreases the expression levels of pro-inflammatory cytokines (13). Based on this information, in the present study, it was hypothesized that EA may exert antitumorigenic effects in NSCLC.

In the present study, A549 human non-small cell lung adenocarcinoma cells were utilized, one of the most widely used models for testing anti-NSCLC compounds. The effects of EA on the proliferation, apoptosis, and the migratory and invasive ability of NSCLC cells were investigated, as well as the mechanisms underlying these effects. Furthermore, athymic nude mice were transplanted with A549 cells in order to establish a xenograft tumor model of NSCLC; it was therefore possible to determine the anti-NSCLC activity of EA *in vivo*. The results presented herein suggest that EA is a potential therapeutic agent against NSCLC.

Materials And Methods

Reagents and antibodies. EA was purchased from Nanjing Spring & Autumn Biological Engineering Co. Ltd., with a purity >98% and dissolved in DMSO (the concentrations used *in vitro* were 10^{-6} M and 10^{-5} M; and those used *in vivo* were 25 and 50 mg/kg via intraperitoneal injection). Rabbit cyclin D polyclonal antibody (1:1,000; cat. no. ABE52), rabbit β-actin polyclonal antibody (1:5,000; cat. no. SAB3500350), rabbit anti-PI3K (1:1000; cat. no. SAB5500162), rabbit anti-partitioning defective 3 homolog (Par3) antibodies (1:1,000; cat. no. SAB1401772), rabbit anti-Bcl-2 (1:1,000; cat. no. SAB4301440), rabbit anti-Bax (1:1,000; cat. no. SAB5700840), rabbit anti-cleaved caspase-3 (1:1,000; cat. no. AB3623), rabbit anti-mTOR (1:1,000; cat. no. T2949), rabbit anti-Akt (1:1,000; cat. no. SAB4500797) and rabbit anti-p-Akt (1:1,000; cat. no. SAB4301497) were purchased from Sigma-Aldrich; Merck KGaA. The ECL chemiluminescence system was purchased from Thermo Fisher Scientific, Inc.

Cells and cell culture. The A549 cell line was purchased from The American Type Culture Collection (cat. no. CRM-CCL-185). Cells were cultured with Dulbecco's modified Eagle's medium (DMEM) supplemented with 10% fetal bovine serum (FBS), in a carbon dioxide incubator in which conditions were maintained at 37˚C and 5% CO_2. The cells were sub-cultured and seeded in 6- or 24-well plates. The cells were divided into following groups: The control; EA(L), treated with 10^{-6} M EA; EA(H), treated with 10^{-5} M EA; and the vehicle, treated with DMSO. Cells were treated with EA for 48 h. Finally, the cells were digested using 0.2% trypsin prior to mRNA or protein analysis.

Establishment of NSCLC tumor xenografts in nude mice. All animal protocols were approved by the Medical Animal Ethics Committee of Lanzhou University Second Hospital (Gan X2020J011), and were all performed according to the Federation of Laboratory Animal Science Associations (FELASA) guidelines

for the definition of humane endpoints and the Arrive guidelines for animal care and protection (14). For metastatic tumor models, the specific humane endpoints were as follows: Rapid weight loss or emaciation characterized by anemia, hunched posture, an ungroomed appearance and lethargy. A total of 20 healthy male athymic BALB/c (nu/nu) nude mice were purchased from Beijing Vital River Laboratory Animal Technology Co., Ltd. The mice were 6 weeks of age and weighed 18-20 g. The mice were housed and fed in a specific pathogen-free (SPF) environment with a 12-h light/dark cycle at 22-25˚C, with 50-65% humidity and were provided with sterile food and water day/night. All procedures were performed under aseptic conditions. Prior to the animal experiments, the mice were fed *ad libitum* for 1 week in their new environment.

Cultured cells were washed with phosphate-buffered saline (PBS), and 0.2 ml ($1x10^6$ cells in total) of cell suspension was injected into the skin of the right underarm region of 5 nude mice (per group). The groups were as follows: The control; EA(L), treated with 25 mg/kg EA; EA(H), treated with 50 mg/kg EA; and the vehicle, treated with corn oil. EA was administered to the mice via intraperitoneal injection from the first day at a dose of 25 mg/kg or 50 mg/kg body weight per day, and corn oil served as the vehicle. The tumor sizes were measured every 5 days. After 4 weeks, the mice were sacrificed and the tumors were collected and fixed with 4% paraformaldehyde. For the tumor models, the specific humane endpoints were the following: Rapid weight loss or emaciation characterized by anemia, hunched posture, ungroomed appearance and lethargy. At the end of the study, tumor volume (mm^3) was calculated according to the following formula: Tumor volume = (length x $width^2$)/2. All mice were anesthetized by an intraperitoneal injection of pentobarbital sodium (30 mg/kg) until they lost consciousness and then sacrificed by exsanguination.

Cell Counting Kit-8 (CCK-8) assay. A CCK-8 kit (Dojindo China Co., Ltd.) was used to measure the proliferation of the A549 cells. A total of 1,000 cells in a volume of 100 µl per well were cultured in five replicate wells in a 96-well plate in medium containing 10% FBS. CCK-8 reagent (10 µl) was then added to 90 µl DMEM to generate a working solution, of which 100 µl was added per well followed by incubation at 37˚C for 1.5 h. This assay was performed at 0, 12, 24 and 36 h.

5-Ethynyl-2'-deoxyuridine (EdU) assay. The Cell-Light™ EdU staining kit (Guangzhou Ribobio Co., Ltd.) was used for the *in vitro* labelling of the nuclei of dividing cells. A549 cells were treated with 2 µM tetrafluorophenyl (TFP) and subsequently with 10 µM EdU. After 16 h, the cells were fixed with 4% paraformaldehyde. The cells were then examined under a laser scanning confocal microscope (Zeiss GmbH).

Cell cycle measurement. Propidium iodide (PI) staining was used for cell cycle measurements according to the instructions provide with the commercial kit (P4170; Sigma-Aldrich; Merck KGaA). Briefly, a cell suspension was prepared in PBS, centrifuged at 500 x g at room temperature for 5min, fixed with 70% alcohol at -20˚C overnight, centrifuged at 300 x g at 4˚C for 5 min and collected, and then washed with PBS. PI solution was added to yield a final concentration of 50 µg/ml. This suspension was kept in the

dark for 30 min. DNA binding was measured using flow cytometry, and the data were analyzed using FlowJo software (Version 9, B&D America).

Cell invasion assay. For the cell invasion assay, a Transwell assay was used with Matrigel® as previously described (15). Briefly, A549 cells ($5x10^5$/ml) were re-suspended in serum-free DMEM containing 0.01% bovine serum albumin (BSA; Sigma-Aldrich; Merck KGaA) for an additional 24 h. The upper chamber of the Transwell plate was covered with serum-free DMEM supplemented with 50 mg/l Matrigel, and was then air-dried at 4˚C for 15 min. A total of 50 µl fresh serum-free DMEM containing 10 g/l BSA was subsequently added followed by incubation for 30 min at 37˚C. Following the removal of this medium, 200 µl cell suspension were added to the upper chamber of the Transwell plate (Sigma-Aldrich; Merck KGaA), and 600 µl complete DMEM culture supplemented with 10% FBS (Sigma-Aldrich; Merck KGaA) were added to the lower chamber. Following 48 h of incubation at 37˚C in 5% CO_2, the Transwell plate was then washed with PBS to remove the cells on the upper side of the microporous membrane, followed by fixation in ice-cold alcohol for 30 min. The non-migratory cells were removed from the upper surface of the filter using a cotton swab. Finally, the cells were stained with 0.1% crystal violet (cat. no. C0775; Sigma-Aldrich; Merck KGaA) for 30 .min at room temperature, and then decolorized with 33% acetic acid. The absorbance of eluents was observed at an optical density of 570 nm using a microplate reader (Bio-Rad Laboratories, Inc.).

Cell migration assay. For the cell migration analysis, a wound healing assay was performed as previously described (10). Briefly, A549 cells ($1x10^5$) were seeded in 24-well plates and grown overnight to achieve confluence (80%). The monolayer of cells was scratched using a 20-µl pipette tip in order to create the wound. Floating cells were removed by washing twice with PBS. Subsequently, serum-free DMEM was added to permit wound healing. The rate of wound closure was assessed using images captured after 24 and 48 h. Image analysis was performed under a fluorescence microscope (magnification, x 200) using Image-Pro Plus software version 6.0 (Media Cybernetics, Inc.).

Hoechst 33258 staining assay. After 4 weeks, the mice were sacrificed and the tumors were collected and fixed with 4% paraformaldehyde for 10 min at room temperature. Following washing with PBS two times, the tissues were stained with 0.5 ml of Hoechst 33258 (Beyotime Institute of Biotechnology) for 5 min, and then again washed twice with PBS. The stained nuclei were observed under an Olympus 1X73 fluorescence microscope (Olympus Corporation) using 350 nm for excitation and 460 nm for emission.

Detection of apoptotic cells in tissues. A TUNEL assay kit was used to detect the apoptotic cells. Tissue sections (thickness, 5 µm) were excised and fixed with 4% paraformaldehyde in PBS at room temperature for 24 h. Fixed tissues were embedded in paraffin and stained using a TUNEL kit (cat. no. 11684795910; Roche Diagnostics), according to the manufacturer's protocol, and 6 sections were analyzed for each mouse. The numbers of apoptotic cells and total tumor cells in each section were counted in three randomly selected fields (magnification, x400) using a fluorescence microscope (Nikon TE-2000 U; Nikon Corporation). The apoptosis index (AI) was expressed as the mean percentage of apoptotic cells within the total number of tumor cells for each animal.

DAPI staining. DAPI staining was performed as follows: Briefly, A549 cells were seeded into 6-well plates with 140,000 cells/well and treated with EA for 24 h. The cells were fixed with 4% polyoxymethylene at room temperature for 10 min. The coverslips were equilibrated in PBS, following which 300 µl DAPI (300 nM; cat.no. D9542; Sigma-Aldrich; Merck KGaA) staining solution was added to the coverslips and incubated for 5 min at room temperature. The coverslips were rinsed two times in PBS and viewed using a fluorescence microscope (Nikon TE-2000 U; Nikon Corporation). The normal cell nuclei were faint staining (cells were alive). The apoptotic cell nuclei were brightness

Western blot analysis. The A549 cells from each group were lysed on ice with a tissue or cell protein extraction reagent (cat.no. P0013; Beyotime Institute of Biotechnology) containing a cocktail of 0.1 mM dithiothreitol and proteinase inhibitor. The protein concentration was determined using a BCA kit (Pierce; Thermo Fisher Scientific, Inc.). A total of 100 µg protein fractions were separated via SDS-PAGE (12% gel), and then transferred onto nitrocellulose membranes (EMD Millipore) in Tris-glycine buffer at 100 V for 55 min. The membranes were then blocked with 5% (w/v) non-fat milk powder in Tris-buffer with 0.05% (v/v) Tween-20 (TBST) at room temperature for 2 h. Following overnight incubation at 4˚C with the appropriate primary antibodies [cyclin D, cat. no. ABE52; Par3, cat. no. SAB1401772; PI3K, cat. no. SAB5500162; AKT, cat. no. SAB4500797; mTOR, cat. no. T2949; p-mTOR, cat. no. SAB4504476; Bax, cat. no. B8429; Bcl-2, cat. no. SAB4503899; caspase-3, cat. no. ABC495; cleaved caspase-3, cat. no. AB3623; proliferating cell nuclear antigen (PCNA), cat. no. WH0005111M2; all 1:1,000; all from Sigma-Aldrich; Merck KGaA] and rabbit β-actin polyclonal antibody (1:5,000; cat. no. SAB3500350; Sigma-Aldrich; Merck KGaA), the membranes were washed three times with TBST, incubated with secondary antibodies (1:5,000; cat. no. ab205718; Abcam) for 2 h at room temperature, and then washed again three times with TBST. The western blot bands were imaged using an enhanced chemiluminescence solution (Beyotime Institute of Biotechnology). The protein expression levels were visualized with Image Lab version 2 Software (Bio-Rad Laboratories, Inc.).

Measurement of mRNA expression. Reverse transcription-quantitative PCR (RT-qPCR) was used to analyze the mRNA levels. Total RNA was extracted from the cells using TRIzol® reagent Takara Biotechnology Co., Ltd; the concentration and purity of RNA were determined by spectrophotometry (Thermo Fisher Scientific Varioskan LUX). A total of 200 ng RNA from each sample was used for the reverse transcription reaction, which was conducted according to instructions for a commercial transcription kit (DRR037A; Takara Biotechnology Co., Ltd.). The following thermocycling conditions were used: Initial denaturation at 95˚C for 30 sec; followed by 40 cycles of denaturation at 95˚C for 5 sec, and annellation and extension at 60˚C for 31 sec. Using qPCR, the mRNA expression levels of Par3 (forward, 5'-CAATTACTATTCAAGCCGTTTTGCCCCTGACAGCCAGTAT-3' and reverse, 5'-CAATTACTATTCAAGCCGTTTTGACCCTGACAGCCAGTAT-3';) and cyclinD (forward, 5’-GTCGCTGGAGCCCGTAA-3’ and reverse, 5’-GAGTTGTCGGTGTAG-3’) were quantified using SYBR Premix Ex Taq (Takara Biotechnology Co., Ltd.) and ABI 7300. Data analysis was performed using ABI software (Version 2.3; Thermo Fisher Scientific, Inc.) using the $2^{-\Delta\Delta Cq}$ method (16).

Statistical analysis. SPSS software (version 19.0; SPSS, Inc.) was used for the statistical analysis. Data are expressed as the mean ± standard error of the mean. Differences in measured values among the multiple groups were evaluated using one-way ANOVA with Bonferroni's multiple comparisons correction. $P<0.05$ was considered to indicate a statistically significant difference.

Results

EA inhibits the viability and proliferation of A549 cells. In order to examine the effects of EA on the viability and proliferation of A549 cells, the cell proliferation and viability of A549 cells were determined using CCK-8 assay and EdU staining. As illustrated in Fig. 2, EA significantly decreased A549 cell viability at the concentrations of 10^{-6} and 10^{-5} M. Furthermore, it was also revealed that EA significantly inhibited A549 cell proliferation (Fig. 2B and C). These results thus suggest that EA may exert anti-proliferative effects against the A549 cells.

EA inhibits the migration and invasion of A549 cells. In order to investigate whether EA may be an effective antitumor agent, the migratory and invasive abilities of the A549 cells were measured using wound healing and Transwell assays. As presented in Fig. 3, EA significantly inhibited the migration of A549 cells at the concentrations of 10^{-6} and 10^{-5} M. As revealed using Transwell assay, EA also significantly decreased A549 cell invasion (Fig. 3B and D). Thus, these results suggest that EA can inhibit the migratory and invasive ability of A549 cells.

EA affects the cell cycle of A549 cells. In order to investigate whether EA inhibits proliferation of A549 cells, distributions of different growth phases were determined using a flow cytometer. As presented in Fig. 4A and B, EA significantly increased the percentage of cells in the G_1 phase, and decreased the percentage of cells in the S and G_2 phases. In addition, as cyclin D plays an important role in cell cycle regulation and progression, the present study examined the effect of EA on the expression of cyclin D in A549 cells using western blot analysis and RT-qPCR in order to determine the expression levels of cyclin D. As shown in Fig. 4C and D, exposure to EA significantly decreased the expression of cyclin D. These results thus indicate that the potential anti-proliferation mechanism of EA is associated with impeding the cell cycle progression from the G_1 phase and thereby attenuating cell proliferation.

EA upregulates Par3 expression and decreases the phosphorylation of PI3K/Akt/mTOR in A549 cells. Par3 is a molecule that has been reported to be involved in the formation of cell polarity during division, and one that is disrupted in epithelial-derived cancers, such as the A549 lung carcinoma cells (17) used in the present study. Therefore, the present study measured Par3 expression using western blot analysis and RT-qPCR in cells exposed to EA. As illustrated in Fig. 5A and B, EA significantly increased the expression level of Par3 in a concentration-dependent manner.

The PI3K/Akt/mTOR pathway is one of the key pathways involved in tumorigenesis; therefore, the present study also measured the expression levels and phosphorylation of these proteins in cells exposed to EA. EA significantly decreased the phosphorylation levels of PI3K, Akt and mTOR (Fig. 5C-F). These results

thus suggest that EA affects the cell cycle regulation and progression of A549 cells by inhibiting the phosphorylation of PI3K/Akt/mTOR, and by upregulating Par3 expression.

EA downregulates Bcl-2 expression, and upregulates Bax and caspase-3 expression in A549 cells. To investigate whether EA could exert pro-apoptotic effects against A549 cells, the present study hypothesized that this pro-apoptotic action may be associated with the regulation of classic apoptosis-pathway-associated proteins. Therefore, the present study examined the effects of EA on the expression levels of Bcl-2, Bax, cleaved caspase-3 and caspase-3 in A549 cells. As presented in Fig. 6A and B, EA significantly decreased the expression levels of Bcl-2, and increased those of Bax in A549 cells. Conversely, EA significantly increased the expression of cleaved caspase-3 (Fig. 6C and D). Thus, these results suggest that a potential mechanism of the suppressive effects of EA against A549 cells include the regulation of apoptosis.

EA inhibits tumor growth and tumor cell proliferation, and induces tumor cell apoptosis in vivo. The results obtained *in vitro* suggested that EA inhibited tumor cell proliferation and induced tumor cell apoptosis. To determine whether EA also inhibits tumors *in vivo*, the present study examined its effect on tumor growth in athymic nude mice. EA (25 and 50 mg/kg) significantly inhibited the growth of A549-induced tumor tissues, as measured by tumor weight and size (among the tumor tissues, the maximum volume was 810 mm^3) (Fig. 7A-C).

In addition, PCNA is a protein that is associated with the proliferation of numerous tumors, including the NSCLC modeled by A549 cells (18). Therefore, the expression level of PCNA was determined *in vivo*. EA significantly downregulated the expression level of PCNA in the tumor tissues (Fig. 7D).

Hoechst 33258 staining also revealed that EA significantly increased tumor tissue apoptosis *in vivo* (Fig. 7E and F). To further determine whether EA inhibits the body weight of the animals at different time periods, the present study examined the body weight of the mice. No obvious changes in body weight were observed among all groups (Fig. 7G). Furthermore, it was found that EA exerted no effects in non-tumor tissue (Fig. 7H). Taken together, these results suggest that EA inhibits tumor cell proliferation and induces tumor cell apoptosis *in vivo*.

Discussion

E. prostrata, of the composite family, commonly known as ‘false daisy’, is an herb that is widely distributed throughout tropical and subtropical countries in Asia. For several years in Asia, *E. prostrata* has been widely used in the treatment of infectious hepatitis, liver cirrhosis, jaundice, aching, and the weakness of the knees and joints, hematuria, abnormal uterine bleeding and diarrhea with bloody stools (19). It has been reported to exert hepatoprotective (20), hypolipidemic (21), immunomodulatory (22), analgesic (23), anti-venom (24), antioxidant (25), anti-inflammatory (26) and anti-aging (27) effects. However, the majority of studies on the biological activities of the plant have been conducted using crude extracts. The phytochemical studies on *Eclipta* species have revealed the presence of a wide range of

bioactive compounds, such as thiophenes, alkaloids, flavonoids, coumestans and triterpenes (28). Although the anticancer activity of *E. prostrata* has been suggested (7, 8, 29), the tumoricidal and antitumorigenic activity of compounds isolated from *E. prostrata* in human cancer cells, and the underlying molecular mechanisms of action of any such activity, have remained largely unknown.

Triterpenes are biosynthesized by the cyclization of squalene in plants, animals and fungi, and are also referred to as triterpenoids. These compounds, such as ursolic acid, betulinic acid and oleanolic acid, have been found to induce the apoptosis of several human cancer cell types (6). EA, a triterpene isolated from *E. prostrata*, has exhibited potent anticancer activity. Tong *et al* (7) investigated the anticancer activity of EA on human hepatoblastoma (HepG2 cells), and revealed that EA induced the apoptosis of HepG2 cells, as characterized by DNA fragmentation, the activation of caspase-3, -8 and -9, and PARP cleavage. EA also induced the loss of mitochondrial membrane potential and induced cytochrome *c* release from the mitochondria to the cytosol. It was also suggested that JNK- and p38 kinase-mediated mitochondrial pathways may be involved in EA-induced HepG2 apoptosis (7). Similar results have been demonstrated in human promyelocytic leukemia cells (HL-60); EA induces HL-60 cellular apoptosis through a ROS-independent mitochondrial dysfunction pathway (8). Recently, the cytotoxic activity of EA in human ovarian and endometrial cancer cells (SKOV3, A2780, OVCAR3, HEC1A and Ishikawa) was investigated. The results revealed that EA significantly inhibited the proliferation of these cancer cells (9, 29).

The present study further investigated the anticancer activity of EA in NSCLC, and found that EA suppressed the proliferation of A549 cells. The migratory and invasive abilities of the A549 cells were also inhibited by EA. EA significantly increased the percentage of cells in the G_1 phase, and decreased the percentages of cells in the S and G_2 phases of the cell cycle. Furthermore, exposure to EA downregulated the expression of cyclin D1, suggesting that EA induced cycle arrest in the G_1 phase. In addition, *in vivo* experiments using athymic mice indicated that EA significantly decreased tumor size and weight, and suppressed the proliferation of and induced the apoptosis of A549 cells in NSCLC tumor xenografts.

In mammals, the Par family of cell polarity proteins, including Par1, Par3, Par4, Par5, Par6 and PKC, plays key roles in numerous aspects of the cell cycle and organization, such as polarization, migration and proliferation. The Par complex member Par3 has been considered a suppressor of invasion and metastasis (30). Knockdown of Par-3 induces breast tumorigenesis and metastasis (31). Par3 is downregulated in lung adenocarcinoma tissues and is associated with higher rates of lymph node metastasis and recurrence. Furthermore, the knockdown of Par3 promotes lung adenocarcinoma cell proliferation, cell migration, tumor formation and metastasis (32). Notably, it has been reported that Par3 is the only Par subtype detected in A549 cells (33). These studies suggest the key role of Par3 in A549 cell proliferation, migration and metastasis. Given these considerations, the present study examined the effects of EA on the expression level of Par3 in A549 cells, and revealed that treatment with EA upregulated Par3 expression. This observation suggests that the mechanism of inhibition of A549 cell proliferation, migration and invasion by EA involves Par3 upregulation.

The PI3K/Akt/mTOR signaling pathway is one of the most frequently dysregulated signaling pathways, which is associated with various aspects of cellular functions. It has been demonstrated that the PI3K/Akt/mTOR signaling pathway is targeted for cancer prevention and intervention (34, 35). The oncogenic activation of the pathway is involved in cancer initiation and progression, including cellular growth, proliferation, drug resistance and survival (36). The activated p-Akt protein is translocated into the cytoplasm or nucleus, where it further phosphorylates a series of substrates that may regulate mechanisms including protein synthesis and gene transcription (37). It is noteworthy that Akt can activate mTOR by directly phosphorylating the ser2448 site of mTOR, and thereby regulates the survival or apoptosis of cells (38). Thus, inhibitors of the PI3K/Akt/mTOR pathway have been intensively investigated for anticancer therapies (39, 40). On this basis, the present study investigated the effects of EA on the PI3K/Akt/mTOR signaling pathway, and revealed that EA significantly inhibited the phosphorylation of PI3K, Akt and mTOR, suggesting that the PI3K/Akt/mTOR pathway is involved in the anti-NSCLC activity of EA.

It has been demonstrated that the water solubility of EA is poor (41–43). It has been well established that poor water solubility leads to low bioavailability, which finally limits the clinical application. The chemical structural modification of EA may improve its water solubility. However, the structure of EA is characterized by a stable ring system and few active sites, which brings great difficulties for structural modification. Therefore, the bioavailability improvement of EA must be completed through formulation modification. Moreover, to determine that the PI3K/Akt/mTOR pathway mediates the anti-NSCLC activity of EA, the use of a PI3K inhibitor or shRNA is required and thus further studies using such methods are warranted. Only one cell line used in present study may be another limitation of the present study; one cell line cannot fully model the NSLCL. As NSCLC is a heterogeneous cancer, two or more cell lines need to be used for provide more convincing results. Thus, further studies are required in order to use other interventions to explore the effects of EA on cell apoptosis and proliferation on other cell lines.

To the best of our knowledge, the present study provides evidence the first time that EA induces the apoptosis, and inhibits the proliferation, migration and invasion ability of A549 cells by increasing Par3 expression and suppressing the PI3K/Akt/mTOR pathway. It was also found that EA inhibits the tumor growth of NSCLC *in vivo*. These findings suggest that EA may represent a potential therapeutic agent for the treatment of NSCLC.

Declarations

Acknowledgements

Not applicable.

Funding

The present study was supported by the Gansu Provincial Technological Science Foundation of China (Grant no. 1606RJZA040) and the Longyuan Youth Innovation and Entrepreneurship Talents (Team)

Project (Grant no. PF2128001)

Availability of data and materials

The datasets used and/or analyzed during the current study are available from the corresponding author on reasonable request.

Authors' contributions

DZ designed and performed experiments, and analyzed, interpreted and presented the results for group discussions. BL, JY and XW were involved in the study methodology, in the description and analysis of the results, and prepared the figures for the manuscript. DZ, BL, JY, XW and CW provided the rationale, background and framework of the study, and also provided feedback regarding the study. DZ and CW confirm the authenticity of all the raw data. DZ, BL, JY, XW and CW have read and approved the final manuscript.

Ethics approval and consent to participate

All animal protocols were approved by the Medical Animal Ethics Committee of Lanzhou University Second Hospital (Gan X2020J011), and were all performed according to the Federation of Laboratory Animal Science Associations (FELASA) guidelines for the definition of humane endpoints and the Arrive guidelines for animal care and protection (13).

Patient consent for publication

Not applicable.

Competing interests

The authors declare that they have no competing interests.

References

1. Gallant JN, Lovly CM. Established, emerging and elusive molecular targets in the treatment of lung cancer. J Pathol. 2018;244:565–77.
2. Fiordoliva I, Meletani T, Baleani MG, Rinaldi S, Savini A, Di Pietro Paolo M, Berardi R. Managing hyponatremia in lung cancer: latest evidence and clinical implications. Ther Adv Med Oncol. 2017;9:711–9.
3. Jung CY, Antonia SJ. Tumor Immunology and Immune Checkpoint Inhibitors in Non-Small Cell Lung Cancer. Tuberc Respir Dis (Seoul). 2018;81:29–41.
4. Mathew M, Enzler T, Shu CA, Rizvi NA. Combining chemotherapy with PD-1 blockade in NSCLC. Pharmacol Ther. 2018;186:130–7.

5. Tseng CY, Lin CH, Wu LY, Wang JS, Chung MC, Chang JF, Chao MW. Potential combinational anti-cancer therapy in non-small cell lung cancer with traditional chinese medicine Sun-Bai-Pi extract and cisplatin. PLoS ONE. 2016;11:e0155469.
6. Chudzik M, Korzonek-Szlacheta I, Krol W. Triterpenes as potentially cytotoxic compounds. Molecules. 2015;20:1610–25.
7. Tong X, Lin S, Fujii M, Hou DX. Molecular mechanisms of echinocystic acid-induced apoptosis in HepG2 cells. Biochem Biophys Res Commun. 2004;321:539–46.
8. Tong X, Lin S, Fujii M, Hou DX. Echinocystic acid induces apoptosis in HL-60 cells through mitochondria-mediated death pathway. Cancer Lett. 2004;212:21–32.
9. Lee J-S, Ahn J-H, Cho Y-J, Kim H-Y, Yang Y-I, Lee K-T, Jang D-S. Jung-Hye Choi. α-Terthienylmethanol, Isolated From Eclipta Prostrata, Induces Apoptosis by Generating Reactive Oxygen Species via NADPH Oxidase in Human Endometrial Cancer Cells. J Ethnopharmacol. 2015;169:426–34.
10. Kim H-Y, Kim HM, Ryu B, Lee J-S, Choi J-H. Dae Sik Jang. Constituents of the Aerial Parts of Eclipta Prostrata and Their Cytotoxicity on Human Ovarian Cancer Cells in Vitro. Arch Pharm Res. 2015;38(11):1963–9.
11. Wang T, Si XQ, Zhou GL, Dai R, Zhou G, Cao D, Yang C. In vivo anti-tumor effect and in vitro anti-angiogenic effect of alcohol extract from Euphorbia prostrata. Zhongguo Zhong Yao Za Zhi. 2017;42(9):1722–1729.
12. Shumin Ding X, Hou F, Wang G, Wang X, Tan Y, Liu Y, Zhou H, Qiu E, Sun N, Jiang Z, Li J, Song. Liang Feng, Xiaobin Jia. Regulation of Eclipta prostrata L. components on cigarette smoking-induced autophagy of bronchial epithelial cells via keap1-Nrf2 pathway. Environ Toxico. 2018 May 4.
13. Joh EH, Gu W, Kim DH. Echinocystic acid ameliorates lung inflammation in mice and alveolar macrophages by inhibiting the binding of LPS to TLR4 in NF-kappaB and MAPK pathways. Biochem Pharmacol. 2012;84:331–40.
14. Workman P, Aboagye EO, Balkwill F, Balmain A, Bruder G, Chaplin DJ, Double JA, Everitt J, Farningham DAH, Glennie MJ, Kelland LR, Robinson V, Stratford IJ, Tozer GM, Watson S, Wedge SR, Eccles SA. An ad hoc committee of the National Cancer Research Institute. Guidelines for the welfare and use of animals in cancer research. Br J Cancer. 2010;102:1555–77.
15. Zhou J, Zhou W, Kong F, Xiao X, Kuang H, Zhu Y. microRNA-34a overexpression inhibits cell migration and invasion via regulating SIRT1 in hepatocellular carcinoma. Oncol Lett. 2017;14:6950–4.
16. Livak, Schmittgen. Analysis of relative gene expression data using real-time quantitative PCR and the 2-ΔΔCq method. Methods. 2001;25:402–8.
17. Song T, Tian X, Kai F, Ke J, Wei Z. Li Jing-Song, Wang Si-Hua, Wang Jian-Jun .Loss of Par3 promotes lung adenocarcinoma metastasis through 14-3-3ζ protein. Oncotarget. 2016;7(39):64260–73.
18. Wang L, Kong W, Liu B, Zhang X. Proliferating cell nuclear antigen promotes cell proliferation and tumorigenesis by up-regulating STAT3 in non-small cell lung cancer. Biomed Pharmacother. 2018;104:595–602.

19. Ogunbinu AO, Flamini G, Cioni PL, Ogunwande IA, Okeniyi SO. Essential oil constituents of Eclipta prostrata (L.) L. and vernonia amygdalina delile. Nat Prod Commun. 2009;4:421–4.
20. Lee MK, Ha NR, Yang H, Sung SH, Kim GH, Kim YC. Antiproliferative activity of triterpenoids from Eclipta prostrata on hepatic stellate cells. Phytomedicine. 2008;15:775–80.
21. Dhandapani R. Hypolipidemic activity of Eclipta prostrata (L.) L. leaf extract in atherogenic diet induced hyperlipidemic rats. Indian J Exp Biol. 2007;45:617–9.
22. Liu X, Jiang Y, Zhao Y, Tang H. [Effect of ethyl acetate extract of Eclipta prostrata on mice of normal and immunosupression]. Zhong Yao Cai. 2000;23:407–9.
23. Sawant M, Isaac JC, Narayanan S. Analgesic studies on total alkaloids and alcohol extracts of Eclipta alba (Linn.) Hassk. Phytother Res. 2004;18:111–3.
24. Mors WB, do Nascimento MC, Parente JP, da Silva MH, Melo PA, Suarez-Kurtz G. Neutralization of lethal and myotoxic activities of South American rattlesnake venom by extracts and constituents of the plant Eclipta prostrata (Asteraceae). Toxicon. 1989;27:1003–9.
25. Kim DI, Lee SH, Choi JH, Lillehoj HS, Yu MH, Lee GS. The butanol fraction of Eclipta prostrata (Linn) effectively reduces serum lipid levels and improves antioxidant activities in CD rats. Nutr Res. 2008;28:550–4.
26. Tewtrakul S, Subhadhirasakul S, Tansakul P, Cheenpracha S, Karalai C. Antiinflammatory constituents from Eclipta prostrata using RAW264.7 macrophage cells. Phytother Res. 2011;25:1313–6.
27. Xia X, Yu R, Wang X, Wei M, Li Y, Wang A, Ma Y, Zhang J, Ji Z, Li Y, Wang Q. Role of *Eclipta prostrata* extract in improving spatial learning and memory deficits in D-galactose-induced aging in rats. J Tradit Chin Med. 2019;39(5):649–57.
28. Zhang JS, Guo QM. Studies on the chemical constituents of Eclipta prostrata (L). Yao Xue Xue Bao. 2001;36:34–7.
29. Cho YJ, Woo JH, Lee JS, Jang DS, Lee KT, Choi JH. Eclalbasaponin II induces autophagic and apoptotic cell death in human ovarian cancer cells. J Pharmacol Sci. 2016;132:6–14.
30. Goldstein B, Macara IG. The PAR proteins: fundamental players in animal cell polarization. Dev Cell. 2007;13:609–22.
31. McCaffrey LM, Montalbano J, Mihai C, Macara IG. Loss of the Par3 Polarity Protein Promotes Breast Tumorigenesis and Metastasis. Cancer Cell. 2016;30:351–2.
32. Song T, Tian X, Kai F, Ke J, Wei Z, Jing-Song L, Si-Hua W, Jian-Jun W. Loss of Par3 promotes lung adenocarcinoma metastasis through 14-3-3zeta protein. Oncotarget. 2016;7:64260–73.
33. Seminario-Vidal L, Kreda S, Jones L, O'Neal W, Trejo J, Boucher RC, Lazarowski ER. Thrombin promotes release of ATP from lung epithelial cells through coordinated activation of rho- and Ca2+-dependent signaling pathways. J Biol Chem. 2009;284:20638–48.
34. Aaron C, Tan. Targeting the PI3K/Akt/mTOR pathway in non-small cell lung cancer (NSCLC). Thorac Cancer. 2020;11(3):511–8.

35. Devesh Tewari P, Patni A, Bishayee AN, Sah A. Bishayee. Natural products targeting the PI3K-Akt-mTOR signaling pathway in cancer: A novel therapeutic strategy. Semin Cancer Biol. 2019;S1044-579X(19)30405-5.
36. McCubrey JA, Steelman LS, Chappell WH, Abrams SL, Montalto G, Cervello M, Nicoletti F, Fagone P, Malaponte G, Mazzarino MC, Candido S, Libra M, Basecke J, Mijatovic S, Maksimovic-Ivanic D, Milella M, Tafuri A, Cocco L, Evangelisti C, Chiarini F, Martelli AM. Mutations and deregulation of Ras/Raf/MEK/ERK and PI3K/PTEN/Akt/mTOR cascades which alter therapy response. Oncotarget. 2012;3:954–87.
37. Ildiko Krencz A, Sebestyen. Andras Khoor. mTOR in Lung Neoplasms. Pathol Oncol Res. 2020;26(1):35–48.
38. Cheng H, Shcherba M, Pendurti G, Liang Y, Piperdi B, Perez-Soler R. Targeting the PI3K/AKT/mTOR pathway: potential for lung cancer treatment. Lung Cancer Manag. 2014;3:67–75.
39. Mengqiu Song, Ann M, Bode Z, Dong. Mee-Hyun Lee.AKT as a Therapeutic Target for Cancer. Cancer Res. 2019;79(6):1019–31.
40. Mohan CD, Srinivasa V, Rangappa S, Mervin L, Mohan S, Paricharak S, Baday S, Li F, Shanmugam MK, Chinnathambi A, Zayed ME. Sulaiman Ali Alharbi, Andreas Bender, Gautam Sethi, Basappa, Kanchugarakoppal S Rangappa. Trisubstituted-Imidazoles Induce Apoptosis in Human Breast Cancer Cells by Targeting the Oncogenic PI3K/Akt/mTOR Signaling Pathway. PLoS ONE. 2016;11(4):e0153155.
41. Sulong X, Wang Q, Si L, Shi Y, Wang H, Yu F, Zhang Y, Li Y, Zheng Y, Zhang C, Wang C, Zhang L. Demin Zhou. Synthesis and anti-HCV entry activity studies of β-cyclodextrin-pentacyclic triterpene conjugates. ChemMedChem. 2014;9(5):1060–70.
42. Zhao Z, Matsunami K, Otsuka H, Shinzato T, Takeda Y, Kawahata M. Kentaro Yamaguchi.Schefflerins A-G, new triterpene glucosides from the leaves of Schefflera arboricola. Chem Pharm Bull (Tokyo). 2010;58(10):1343–8.
43. Morris Keller S, Fankhauser N, Giezendanner M, König F, Keresztes O, Danton O, Fertig L, Marcourt M, Hamburger. Veronika Butterweck, Olivier Potterat. Saponins from Saffron Corms Inhibit the Gene Expression and Secretion of Pro-Inflammatory Cytokines. J Nat Prod. 2021;84(3):630–45.

Figures

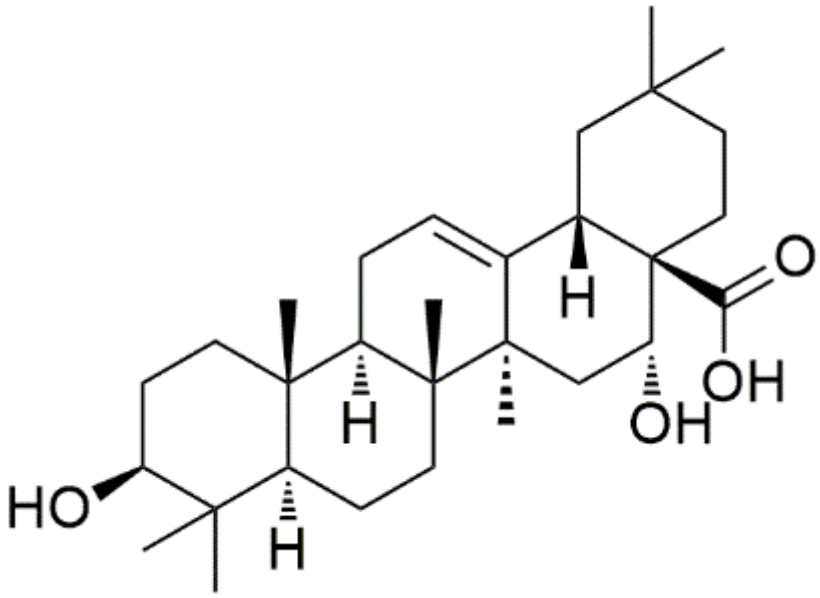

Figure 1

Chemical structure of echinocystic acid

Figure 2

EA inhibits the viability and proliferation of A549 cells. (A) Cell viability measurement. (B) Representative images of EdU staining. (C) Percentage of EdU-positive cells. All values are expressed as the mean ± SEM. *P<0.05 vs. control; **P<0.05 vs. control. EA, echinocystic acid; EA (L), EA at 10^{-6} M; EA (H), EA at 10^{-5} M; vehicle, DMSO; EdU, 5-ethynyl-2’-deoxyuridine.

Figure 3

EA inhibits the migration and invasion of A549 cells. (A) Representative images of wound healing assay. (B) Representative images of Transwell assay. (C) Relative wound width (mm) (gap distance). (D) Relative migration rate. *P<0.05 vs. control; **P<0.05 vs. control. EA, echinocystic acid; EA (L), EA at 10^{-6} M; EA (H), EA at 10^{-5} M; vehicle, DMSO.

Figure 4

EA affects the cell cycle and the expression of cyclin D in A549 cells. (A) Representative images of flow cytometry. (B) Percentage of cells in each phase. (C) Cyclin D mRNA level. (D) Cyclin D protein level. All

values are expressed as the mean ± SEM. *P<0.05 vs. control. EA, echinocystic acid; EA (L), EA at 10^{-6} M; EA (H), EA at 10^{-5} M; vehicle, DMSO.

Figure 5

EA affects the expression of Par3 and the activation of PI3K/Akt/mTOR in A549 cells. (A) Par3 mRNA level. (B) Par3 protein level. (C) Protein level of p-PI3K, PI3K, p-Akt, Akt, p-mTOR and mTOR. (D) Phosphorylation of PI3K. (E) Phosphorylation of Akt. (F) Phosphorylation of mTOR. All values are expressed as the mean ± SEM. *P<0.05 vs. control; **P<0.01 vs. control. EA, echinocystic acid; EA (L), EA at 10^{-6} M; EA (H), EA at 10^{-5} M; vehicle, DMSO.

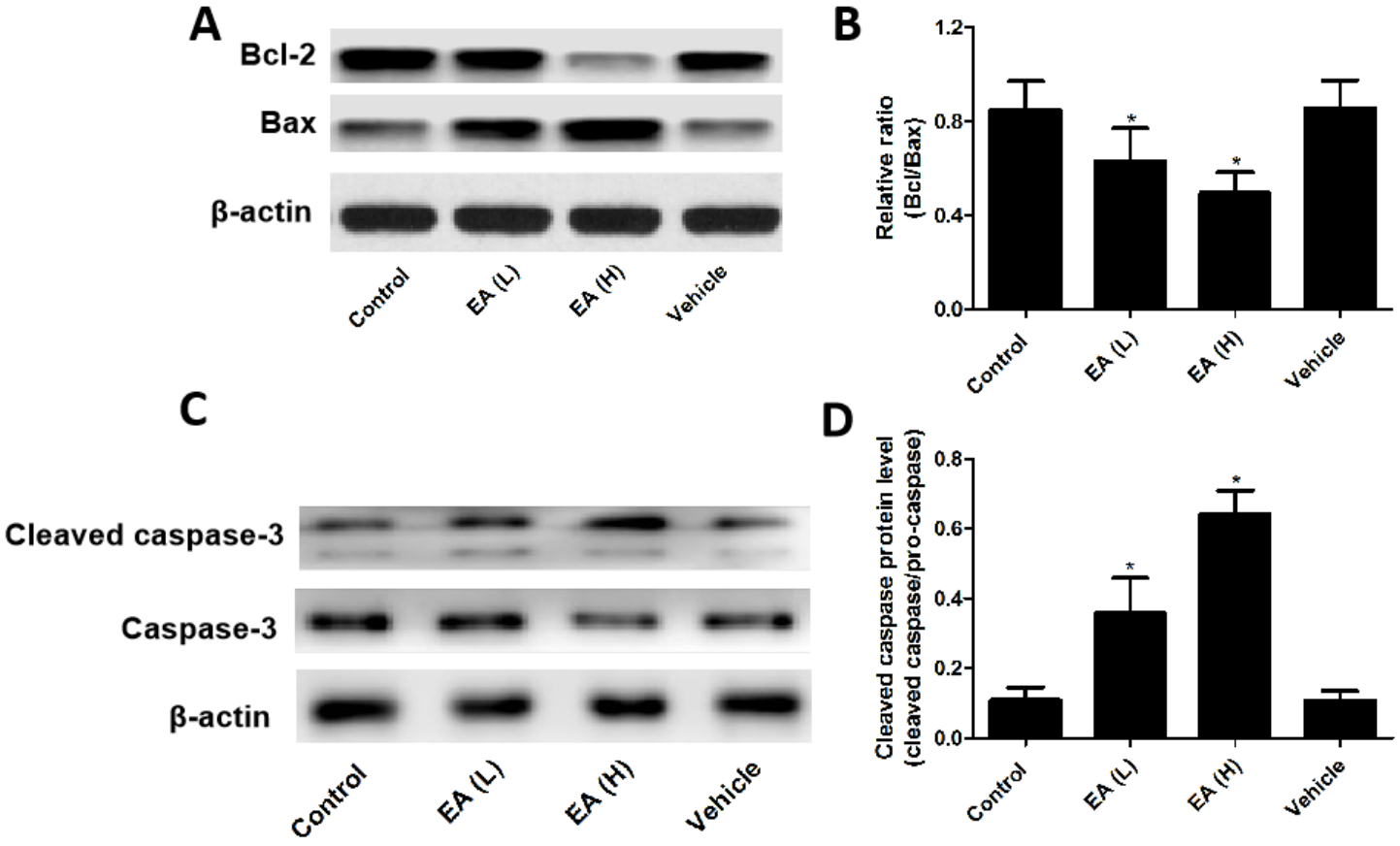

Figure 6

EA affects the expression of Bcl-2, Bax and caspase-3 in A549 cells. (A) Protein expression levels of Bcl-2 and Bax. (B) Relative ratio of Bcl-2/Bax. (C) Protein expression levels of cleaved caspase-3 and caspase-3. (D) Cleaved caspase-3 protein level. All values are expressed as the mean ± SEM. *P<0.05 vs. control. EA, echinocystic acid; EA (L), EA at 10^{-6} M; EA (H), EA at 10^{-5} M; vehicle, DMSO.

Figure 7

EA inhibits tumor growth, inhibits tumor cell proliferation, and induces tumor cell apoptosis *in vivo*. (A) Representative images of tumor tissue. (B) Tumor weight. (C) Tumor size. (D) PCNA protein level. (E) Representative images of TUNEL staining of tumor tissue. (F) Percentage of cells positive for TUNEL staining. (G) Mouse body weights of mice in all groups (n=5 per group). (H) Representative images of TUNEL staining of non-tumor tissue. All values expressed as the mean ± SEM. $^{**}P<0.05$ vs. control; $^{***}P<0.01$ vs. control. EA, echinocystic acid; EA (L), EA at 25 mg/kg; EA (H), EA at 50 mg/kg; vehicle, corn oil.